ACTA SCIENTIAE

ISSN: 2178-7727

Low-Temperature Synthesis and Characterization of Phase-Pure Nanocrystalline BaAl2Ti6O16 Hollandite

Bhimarao M. Patil

Department of Chemistry, The Institute of Science, Mumbai-400032, Maharashtra, India
Corresponding author e-mail address: bmpatilisc77@gmail.com

ABSTRACT

Nanocrystalline BaAl2Ti6O16 (BAT) with a hollandite-type structure was synthesized using a barium aluminum titanyl tartrate (BATT) precursor via a controlled thermal decomposition method. The thermal behaviour of the precursor was studied using simultaneous thermogravimetric and differential thermal analyses (TG–DTA), which revealed a three-step mass loss process associated with dehydration and subsequent decomposition of the tartrate complex. Complete decomposition was achieved at approximately 500°C. X-ray diffraction (XRD) analysis indicated that the product remained amorphous below 700°C, with crystallization into a pure hollandite phase beginning at 800°C. The degree of crystallinity increased progressively up to 1250°C without the formation of any secondary phases. Fourier-transform infrared (FTIR) spectroscopy confirmed the gradual removal of organic moieties and formation of metal–oxygen bonds (Al–O, Ti–O, and Ba–O) during thermal treatment. Particle size distribution and field emission scanning electron microscopy (FE-SEM) studies revealed nanosized crystallites in the range of 27–60 nm, which was further corroborated by transmission electron microscopy (TEM). The SAED patterns confirmed the polycrystalline nature of the synthesized nanoparticles. Dilatometric analysis demonstrated that the shrinkage of the compacted powder commenced above 800°C, while the sintered pellet exhibited a thermal expansion coefficient of 8.80×10^{-6} K^{-1}, consistent with literature values. The density of the sintered pellets exceeded 97% of the theoretical value, highlighting the excellent sinterability of the powder derived from the tartrate route. This study establishes a facile, low-temperature chemical route for producing phase-pure, nanocrystalline $BaAl_2Ti_6O_{16}$ hollandite with desirable thermal and structural stability, suitable for advanced ceramic and nuclear waste immobilization applications.

KEYWORDS: BaAl2Ti6O16, Hollandite, Tartrate precursor, Nanocrystalline ceramics

INTRODUCTION

Nuclear energy is recognized as one of the most promising and sustainable sources for meeting future global energy demands. However, the safe and effective management of high-level nuclear waste (HLW) remains a major challenge associated with nuclear power generation. To address this issue, Ringwood et al. [1-3] proposed a synthetic rock known as SYNROC (synthetic rock), which serves as a durable host matrix for the immobilization of HLW. Among the various crystalline phases constituting SYNROC—perovskite, zirconolite, hollandite, and rutile (TiO_2)—the barium hollandite phase ($BaAl_2Ti_6O_{16}$) plays a particularly important role due to its ability to incorporate large monovalent cations such as cesium within its tunnel-type structure. Cesium (Cs) is one of the major fission products generated during nuclear fuel reprocessing and is of particular concern due to its radioactive isotopes ^{134}Cs and ^{137}Cs (high β and γ activities) and long-lived isotope ^{135}Cs (half-life ≈ 2.3×10^6 years). Immobilization of Cs is challenging because of its high volatility at elevated temperatures, tendency to form water-soluble compounds, and chemical mobility in environmental conditions [4, 5]. During β^- decay, radioactive Cs is transmuted into stable Ba, which can be structurally accommodated within the hollandite lattice [4]. Hence, $BaAl_2Ti_6O_{16}$ (BAT) and related titanate compounds have emerged as promising single-phase host matrices for Cs immobilization owing to their high chemical durability, thermal stability, and strong Cs incorporation capacity [5–8].

Several synthesis routes for $BaAl_2Ti_6O_{16}$ (BAT) have been reported in the literature, including: (i) conventional solid-state ceramic technique [7, 8], (ii) polymerizable complex (Pechini) method [9], (iii)

ISSN: 2178-7727

alkoxide precursor method [4], and (iv) combustion synthesis method [10]. In the conventional solid-state method, $BaAl_2Ti_6O_{16}$ is typically prepared via the reaction between BaO, Al_2O_3, and TiO_2 at temperatures around 1200 °C [7, 8]. However, powders synthesized by this approach often suffer from several limitations, such as high processing temperatures, inhomogeneous mixing of reactants, impurity contamination, and non-uniform particle size distribution.

In order to overcome the drawbacks associated with the conventional ceramic route, various wet-chemical and solution-based synthesis methods have been developed to obtain fine, homogeneous, and chemically pure $BaAl_2Ti_6O_{16}$ powders at relatively lower calcination temperatures. Among these, citrate–nitrate, polymerizable complex (Pechini) and combustion techniques have gained significant attention due to their ability to achieve atomic-level mixing of cations, thereby promoting the formation of a single-phase product at reduced temperatures [4, 9, 10].

In particular, tartrate-based routes are advantageous because they enable controlled chelation of multivalent metal ions, leading to a uniform precursor and improved compositional homogeneity. The use of organic complexing agents such as tartaric acid facilitates polymeric network formation through metal–ligand coordination, which enhances the distribution of cations and minimizes phase segregation during calcination. This results in the formation of nanocrystalline, phase-pure $BaAl_2Ti_6O_{16}$ at significantly lower temperatures compared to conventional solid-state synthesis. Furthermore, the incorporation of barium within the hollandite framework provides structural stability and charge compensation, allowing substitution of Ba^{2+} with Cs^{+} in the tunnel sites without disrupting the framework integrity. This structural feature makes $BaAl_2Ti_6O_{16}$ a potential candidate for immobilizing radioactive cesium, offering excellent thermal, chemical, and radiation stability under repository conditions [11–13].

Therefore, the present work focuses on the synthesis of nanocrystalline $BaAl_2Ti_6O_{16}$ (BAT) using a tartaric acid-assisted chemical route, followed by its thermal, structural, and morphological characterization. The study aims to elucidate the phase evolution behavior, microstructural features, and thermal expansion characteristics of $BaAl_2Ti_6O_{16}$, which are crucial for its application as a durable host matrix for the immobilization of radioactive cesium in nuclear waste management.

MATERIAL AND METHODS

Synthesis of $BaAl_2Ti_6O_{16}$

All chemicals used were of analytical reagent (AnalaR) grade: titanium (III) chloride solution (15% $TiCl_3$, S.D. Fine Chemicals Ltd., Mumbai, India), aluminum nitrate nonahydrate ($Al(NO_3)_3{\cdot}9H_2O$), barium nitrate ($Ba(NO_3)_2$) and tartaric acid (Merck, India).In the synthesis process, equimolar aqueous solutions of $Ba(NO_3)_2$ and $Al(NO_3)_3{\cdot}9H_2O$ were gradually added to the $TiCl_3$ solution under constant stirring. The resulting exothermic reaction facilitated the oxidation of Ti^{3+} to Ti^{4+}, maintaining the overall stoichiometric ratio of Ba:Al:Ti as 1:2:6. During this reaction, the color of the $TiCl_3$ solution changed from violet (Ti^{3+}) to greenish-yellow (Ti^{4+}), confirming oxidation. Subsequently, an aqueous solution of tartaric acid was added to the mixture while maintaining the molar ratio of Ba:Al:Ti:Tartaric acid as 1:2:6:9. The obtained homogeneous solution was then heated in an air oven at 200 °C to yield a free-flowing brown precursor powder. This precursor was subjected to thermal treatment at temperatures ranging from 500 °C to 1250 °C. A single-phase nanocrystalline BAT was obtained through complete thermal decomposition of the precursor at 800 °C for 1 h. A schematic representation of the synthesis steps of BAT is shown in Figure 1. The BAT powder obtained after calcination at 1000 °C for 1 h was finely ground and pelletized under a uniaxial pressure of 50 MPa into pellets of 8 mm diameter and 5 mm thickness. The pellets were sintered in air at 1250 °C for 5 h, with a heating rate of 10 °C min^{-1}.

ISSN: 2178-7727

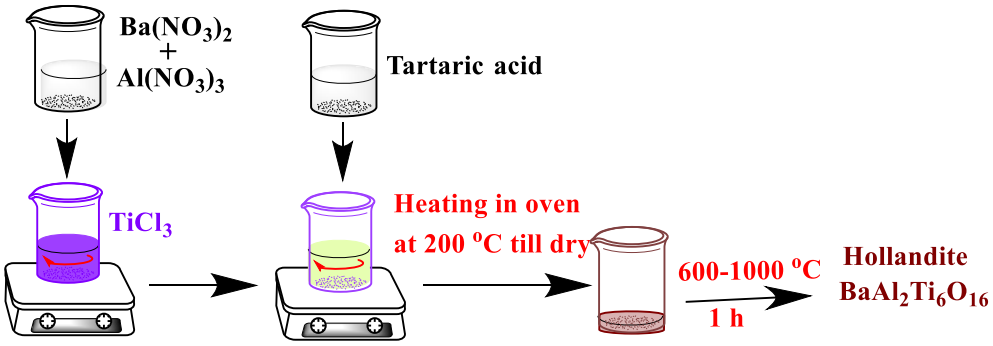

Figure 1: Schematic of the $BaAl_2Ti_6O_{16}$ (BAT) synthesis.

Characterizations

The simultaneous thermogravimetric–differential thermal analysis (TG–DTA) of the precursor was carried out in flowing air using a DIAMOND TG–DTA instrument (PerkinElmer, Germany). The thermal behavior provided insights into the decomposition and phase formation processes of the precursor. The phase composition of the calcined BAT powders obtained after heat treatment at various temperatures was examined by X-ray diffraction (XRD) using a Rigaku Miniflex II X-ray diffractometer equipped with a monochromatic Cu Kα radiation source (λ = 0.15405 nm).

The morphological evolution of BAT samples at different calcination temperatures was investigated using field emission scanning electron microscopy (FE-SEM, JEOL JSM-7600F) and high-resolution transmission electron microscopy (HR-TEM, FEI Tecnai G2 F30, 300 kV). The linear thermal expansion of the sintered BAT pellet was measured in the temperature range of 30 °C to 950 °C at a heating rate of 10 °C min^{-1} using a push-rod thermodilatometer (NETZSCH DIL 402 Classic). The bulk density of the sintered pellets was determined by the Archimedes liquid displacement method.

RESULTS AND DISCUSSION

Thermal Analysis of Barium Aluminum Titanyl Tartrate (BATT) Precursor

The simultaneously recorded thermogravimetric (TG) and differential thermal analysis (DTA) curves of the BATT precursor are presented in Figure 2. The TG curve reveals a three-step mass loss process. The initial mass loss of approximately 8 wt% occurs up to 150°C, corresponding to the removal of adsorbed and coordinated water molecules. This dehydration step is followed by two successive, partially overlapping decomposition steps. Beyond 500°C, no further weight loss is observed, indicating the complete decomposition of the tartrate precursor.

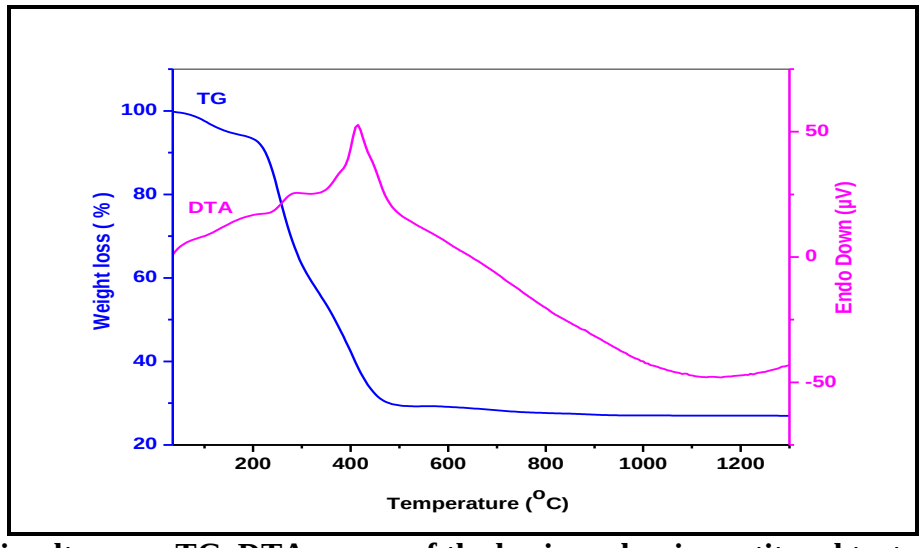

Figure 2. Simultaneous TG–DTA curves of the barium aluminum titanyl tartrate (BATT) precursor.

ISSN: 2178-7727

The DTA curve exhibits a broad exothermic peak in the temperature range of 25–1100°C, with two distinct exothermic features centered around 200°C and 350°C, superimposed on the broader background peak. The latter two peaks are attributed to the oxidation of evolved gases such as CO and H_2 during tartrate decomposition. The broad underlying exothermic peak likely corresponds to the gradual crystallization of the decomposed intermediate phases. The broad exothermic feature observed above 500°C on the DTA curve is therefore associated with the crystallization of the amorphous/glassy intermediate phase. This interpretation is supported by the XRD data of samples annealed at progressively higher temperatures (Figure 3a–h). The formation of crystalline, nanosized $BaAl_2Ti_6O_{16}$ occurs at 800°C.

X-ray Diffraction Analysis of $BaAl_2Ti_6O_{16}$:

The XRD patterns of the products obtained by heating the BATT precursor at various temperatures in air for one hour are shown in Figure 3. The material remains nearly amorphous below 700°C, gradually transforming into a crystalline hollandite-type structure at 800°C (Figure 3e). Further annealing up to 1250°C enhances the crystallinity of the product (Figures 3f–h). Importantly, no additional diffraction peaks are detected, indicating phase purity of the hollandite BAT, which matches the standard JCPDS card No. 33-0133[14, 15]

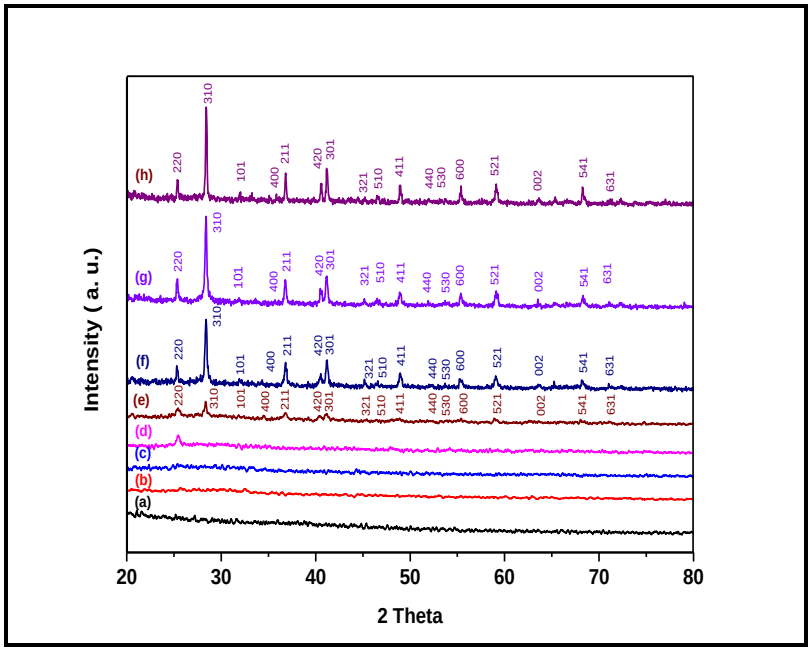

Figure 3. XRD patterns of BATT precursor: (a) as-prepared, (b) 500°C, (c) 600°C, (d) 700°C, (e) 800°C, (f) 900°C, (g) 1000°C, (h) 1250°C (1 h, air atmosphere).

FTIR Spectroscopic Analysis

The FTIR spectra of the BATT precursor and its heat-treated products (500–1250 °C) are presented in Figure 4. The observed absorption bands correspond to various functional groups associated with the tartrate precursor. The bands near 992 cm^{-1} and 1052 cm^{-1} are attributed to the stretching vibrations of Al–O bonds. The spectra demonstrate the gradual removal of organic components and the progressive formation of metal–oxygen bonds with increasing temperature. The broad absorption band around 3437 cm^{-1} is assigned to the O–H stretching vibration of adsorbed water, while the peak near 1635 cm^{-1} corresponds to the C=O stretching of carbonyl groups and the bending vibrations of adsorbed water. In the as-prepared precursor, the band at 1317 cm^{-1} is attributed to C–O stretching vibrations. Upon annealing at 500 °C, new peaks appear at approximately 1486 cm^{-1} and 860 cm^{-1}, likely indicating carbonate formation (Fig. 4b). The intensity of these peaks decreases with increasing temperature, disappearing above 700 °C due to carbonate decomposition. At 800 °C, multiple peaks in the 500–900 cm^{-1} range coalesce into two broad peaks at 793 cm^{-1} and 577 cm^{-1}, consistent with the formation of a single-phase hollandite structure. These FTIR observations are in good agreement with the XRD results discussed earlier, confirming the temperature-dependent structural evolution of the material.

ISSN: 2178-7727

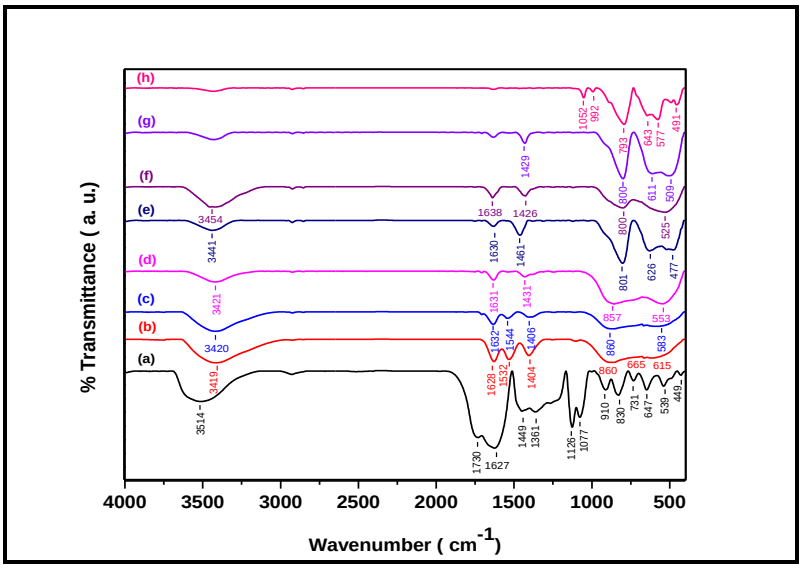

Figure 4. FTIR spectra of BATT precursor: (a) as-prepared, (b) 500°C, (c) 600°C, (d) 700°C, (e) 800°C, (f) 900°C, (g) 1000°C, (h) 1250°C (1 h).

Particle size distribution

The particle size distribution curve for BAT obtained after heating the precursor at 1000°C for 1 h is shown in Figure 5. The majority of particles fall within the 27–60 nm range, as further confirmed by SEM micrographs (Figure 6)

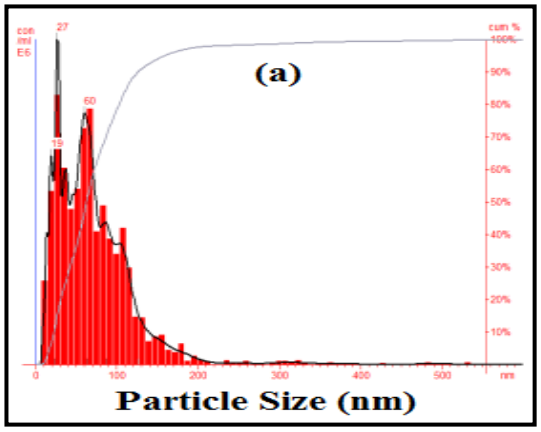

Figure 5. Particle size distribution curve of BAT sample.

Field Emission Scanning Electron Microscopy (FE-SEM) Studies:

FE-SEM micrographs of the $BaAl_2Ti_6O_{16}$ powders obtained at various temperatures are shown in Figure 6. The sample annealed at 700°C (Figure 6a) exhibits a glassy amorphous morphology, while the material treated at 800°C (Figure 6b) begins to develop granular features, indicating the onset of crystallization. At 1000°C (Figure 6c), well-defined nanoparticles (~200 nm) with irregular shapes are observed, which grow further at 1250°C (Figure 6d), consistent with increased crystallinity observed in XRD patterns.

ISSN: 2178-7727

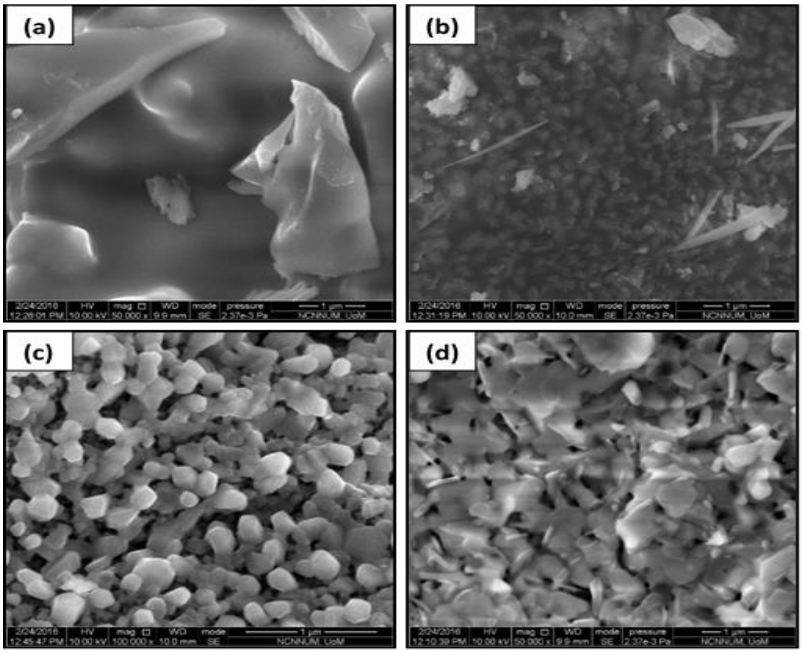

Figure 6. FE-SEM images of BAT powders: (a) 700°C, (b) 800°C, (c) 1000°C, (d) 1250°C (1 h).

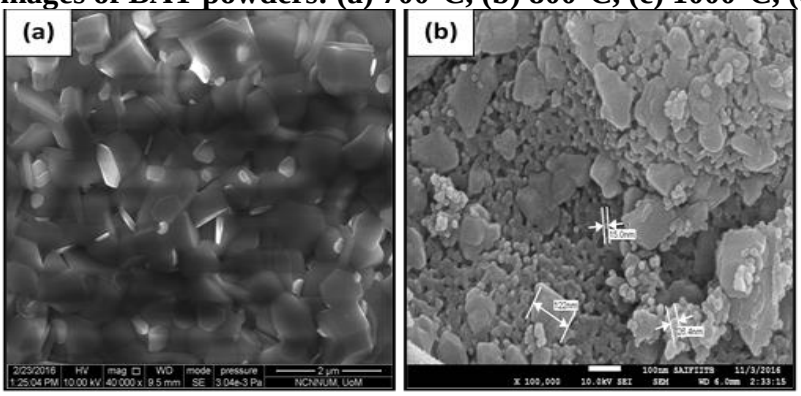

Figure 7. SEM images of BAT (a) sintered pellet, (b) powder (1000°C, 1 h, sonicated),

Pelletized samples sintered at 1250°C for 5 h (Figure 7a) show enhanced densification compared to powder samples. Figure 7b displays the microstructure of the powder annealed at 1000°C and subsequently sonicated in distilled water for 5 minutes, revealing closely packed nanocrystals. The corresponding SEM image (Figure 7b) confirms particle sizes ranging from 15 to 122 nm, aligning with the nanoparticle analyzer data.

Transmission Electron Microscopy (TEM) and SAED Analysis

TEM and selected area electron diffraction (SAED) patterns of $BaAl_2Ti_6O_{16}$ synthesized at 1000°C for 1 h, followed by 5 min sonication in deionized water, are presented in Figure 8. The particles consist of numerous nanocrystals ranging from 50–100 nm, with occasional particles smaller than 50 nm and larger than 200 nm. The ring-like SAED patterns confirm the polycrystalline nature of the nanoparticles. Sonication likely contributes to the fragmentation of agglomerated particles into discrete nanocrystallites.

ISSN: 2178-7727

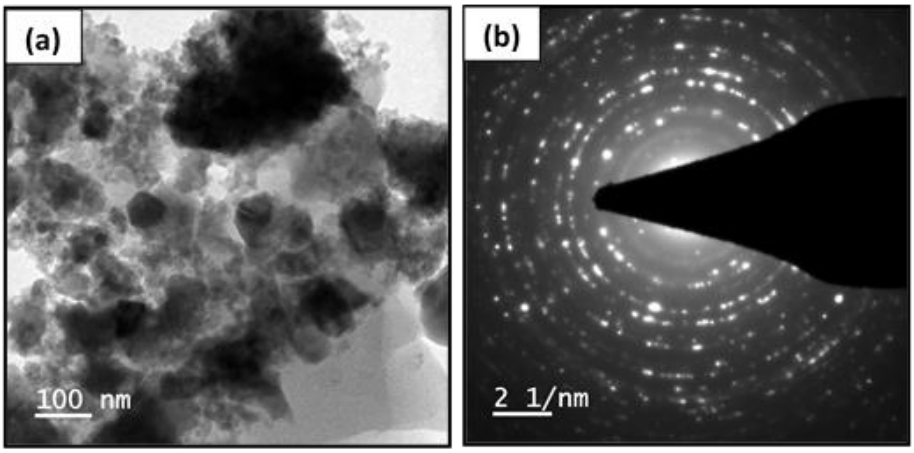

Figure 8. (a) TEM image and (b) SAED pattern of BAT powder (1000°C, 1 h, sonicated).

Shrinkage and Thermal Expansion Behavior

The shrinkage behavior of cold-pressed BAT pellets was studied using a thermodilatometer to optimize the sintering temperature (Figure 9). The green pellets begin to shrink above 800°C, indicating this as the onset temperature for sintering. Consequently, 1250°C was chosen as the sintering temperature to achieve rapid densification.

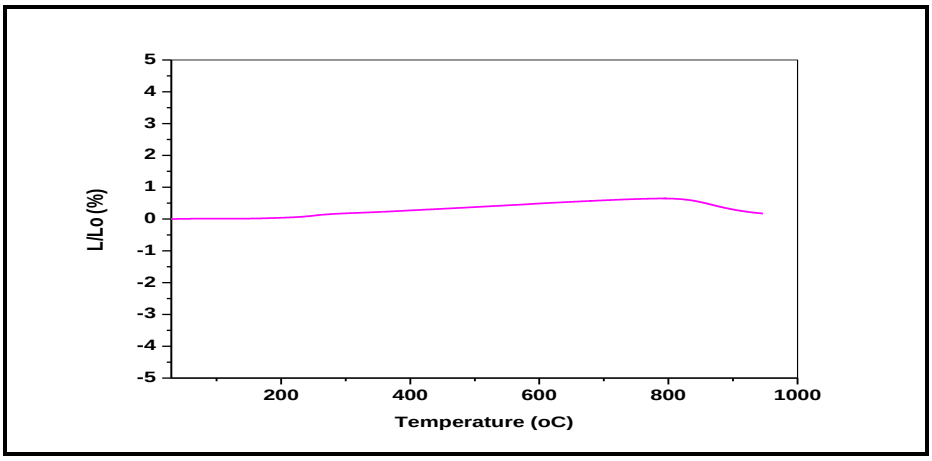

Figure 9. Shrinkage pattern of BAT green pellet.

The bulk thermal expansion behavior of sintered BAT pellets is shown in Figure 10. The measured linear thermal expansion coefficient ($\alpha = 8.80 \times 10^{-6}\ K^{-1}$) agrees well with values reported by Muthuraman et al. [12] and Hoenig et al. [13].

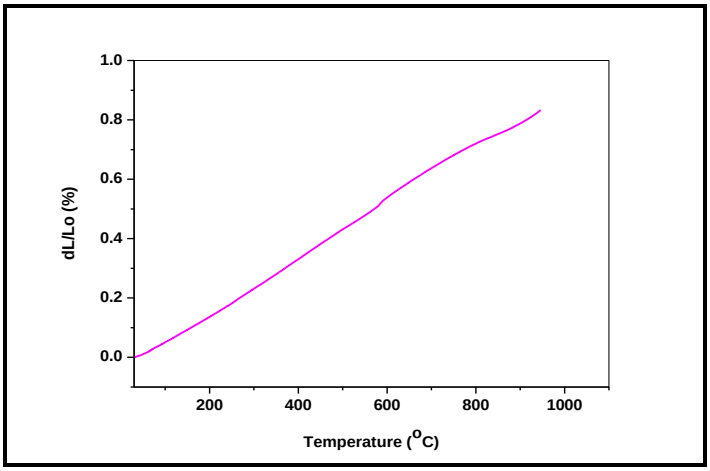

Figure 10. Thermal expansion of sintered BAT pellet.

ISSN: 2178-7727

Density Determination:
The density of sintered hollandite pellets was determined using the liquid displacement method in benzene and carbon tetrachloride. The samples achieved a relative density exceeding 97% of the theoretical value after sintering at 1250°C for 5 h, demonstrating excellent sinterability of the $BaAl_2Ti_6O_{16}$ powder derived from the tartrate precursor.

CONCLUSION

The present study demonstrates an efficient tartrate precursor route for synthesizing phase-pure $BaAl_2Ti_6O_{16}$ hollandite nanoceramics. Thermal analysis (TG–DTA) confirmed stepwise dehydration, oxidation, and crystallization, with complete phase formation occurring at 800°C. XRD and FTIR analyses verified the removal of organic moieties and development of metal–oxygen bonding. Microstructural studies (FE-SEM, TEM) revealed uniformly distributed, polycrystalline nanoparticles in the 27–60 nm range. Optimal sintering above 800°C yielded dense pellets (≥97% theoretical density) with a thermal expansion coefficient of 8.8×10^{-6} K^{-1}. Overall, the tartrate precursor route offers a simple, reproducible, and energy-efficient method to obtain fine-grained hollandite $BaAl_2Ti_6O_{16}$ ceramics, making it suitable for functional applications in high-temperature electronics and immobilization of radioactive waste materials.

ACKNOWLEDGMENTS

The author would like to acknowledge Dr. Pravin Walke, Centre of nanoscience and Nanotechnology for SEM images, SAIF, IIT, Mumbai for TG-DTA, FTIR spectra, Dilatometry study and TEM images and Dr. S. R. Dharwadkar for valuable guidance

REFERENCES:

1. A. E. Ringwood, S. E. Kesson, N. G. Ware, W. Hibberson, and A. Major, Immobilization of high-level nuclear waste in SYNROC, Nature, 278 (5701) (1979) 219.
2. A. E. Ringwood, S. E. Kessom, N. G. Ware, W. O. Hibberson, and A. Major, The SYNROC process: A geochemical approach to nuclear waste immobilization, A. Geochemical Journal, 13 (1979) 141.
3. A. E. Ringwood, V. M. Oversby, S. E. Kesson, W. Sinclair, N. Ware, W. Hibberson, A. Major, Nucl. Chem. Waste Manag., 2 (4) (1981) 287.
4. A.Y. Leinkugel-le-Cocq, P. Deniard, S. Jobie, R. Cerny, F. Bart, and H. Emerich, Synthesis and characterization of hollandite-type material intended for the specific containment of radioactive cesium, J. Solid State Chem, 179 (10) (2006) 3196.
5. J. Amoroso, J. Marra, S. D. Conradson, M. Tang, and K. Brinkman, Microstructures of Melt-Processed and Spark Plasma Sintered Ceramic Waste Forms, J. Alloys Compd., 584 (2014) 590.
6. M. Watanabe, Y. Fujiki, Y. Kanazawa, and K. Tsukimura, The effects of cation substitution on the hollandite-type structure, J. Solid State Chem., 66 (1) (1987) 56.
7. I. W. Donald, B. L. Medtacalfe and K. N. J. Taylor, The immobilization of high level radioactive wastes using ceramics and glasses, J. Mater. Sci., 32 (22) (1997) 5851.
8. R. W. Cheary, An X-ray structural analysis of cesium substitution in the barium hollandite phase of synroc, J. Nucl. Mater., 125 (1984) (2007) 236.
9. H. Xu, G. C. C. Costa, C. R. Stanek and A. Navrotsky, Structural Behavior of $Ba_{1.24}Al_{2.48}Ti_{5.52}O_{16}$ Hollandite at High Temperature: An In Situ Neutron Diffraction Study, J. Am. Cream. Sco., 98 (2015) 255.
10. M. Muthuraman, N. A. Dhas, and K. C. Patil, Combustion synthesis of oxide materials for nuclear waste immobilization, Bull. Mater. Sci., 17 (6) (1994) 977.
11. Mohsen A. Asadabad and Mohammad J. Eskandari, Modern Electron Microscopy in Physical and Life Science. INTECH, Open Science/ Open Minds, (2016).
12. M. Muthuraman, K.C. Patil, S. Senbagaraman, and A.M. Umarji, Sintering, microstructural and dilatometric studies of combustion synthesized synroc phases, Mater. Res. Bull, 31 (11) (1996) 1375.
13. C. L. Hoenig, H. W. Newkirk, R. A. Otto, R. L. Brady, A. E. Brown, A. R. Ulrich, R. C. Lum, Mechanical and Thermophysical Properties of Hot-Pressed SYNROC B, Lawrence Livermore Laboratory, University of California, Livermorc, California, 1-15 (1981).

ISSN: 2178-7727

14. H.S. Potdar, S. Vijayanad, K. Khaja Mohaideen, K.R Patiul, P.A. Joy, R. Raja Madhavan, K.v.G. Kutty, R.D. Ambashta and P.K. Wattal, A simple chemical co-precipitation/calcination route for the synthesis of simulated synroc-B and synroc-C powders, Mater. Chem.Phys., 123 (2) (2010) 695.
15. Y.M. Han, S. J. Lee, Y.K. Kim and C.H. Jung, Synthesis of Nano-Polycrystalline Synroc-B Powders as a High-Level Radioactive Wastes Ceramic Forms by a Solution Combustion Synthesis, J. Nanosci. Nanotechnol., Vol (2) (2016) 1672.